Co-assembly of Plasma and Cellular Fibronectins into Fibrils in Human Fibroblast Cultures

Donna M. Pesciotta Peters,* Lisa M. Portz,* Jan Fullenwider,§ and Deane F. Mosher‡§

Departments of *Pathology, ‡Medicine, and §Physiological Chemistry, University of Wisconsin, Madison, Wisconsin 53706

Abstract. Exogenous plasma and endogenous cellular fibronectins on the surface of cultured fibroblasts and in extracellular matrix fibrils were colocalized by fluorescent and high voltage immunoelectron microscopy. Fibroblast cultures grown in the presence or absence of cycloheximide were incubated with exogenous plasma fibronectin labeled with fluorescein isothiocyanate. A monoclonal antibody specific for the EIIIA sequence of cellular fibronectin was used to detect cellular fibronectin. A rabbit antifluorescein antibody identified fluoresceinated plasma fibronectin. In cultures incubated in the presence of cycloheximide, plasma fibronectin was bound to the cell surface and was assembled into extracellular fibrils. In cultures grown in the absence of cycloheximide, plasma and cellular fibronectins were observed in the same matrix fibrils and in the same locations on the cell surface. There was not, however, random admixture of the two proteins.

FIBRONECTIN is a multifunctional glycoprotein that can be found in a fibrillar network in the extracellular matrix of connective tissues, basement membranes and cultured cells. There are at least 20 different forms of fibronectin that can be generated by alternative mRNA splicing of nascent mRNA (Schwarzbauer et al., 1983, 1987*a*; Kornblihtt et al., 1984, 1985). Plasma fibronectin (pFN)[1] differs from cellular fibronectin (cFN) in that it is missing completely two type III sequences (EDIIIA and EDIIIB) found in a portion of cFN subunits (Gutman and Kornblihtt, 1987; Schwarzbauer et al., 1987*a*; Zardi et al., 1987). Both pFN and cFN can be found in tissues and in extracellular matrix fibrils of fibroblasts cultured in serum (Hayman and Ruoslahti, 1979; Oh et al., 1981).

The incorporation of fibronectin into fibrils occurs principally at the cell surface (McKeown-Longo and Mosher, 1983) and requires the amino terminal portion of the molecule (McKeown-Longo and Mosher, 1985; McDonald et al., 1987; Schwarzbauer et al., 1987*b*; Quade and McDonald, 1988) and the cell adhesion domain (McDonald et al., 1987; Roman et al., 1989). Both labeled pFN and cFN bind to the cell layer in two fractions, a deoxycholate-soluble fraction (cell surface fraction) and a deoxycholate-insoluble (extracellular matrix) fraction containing disulfide bonded fibronectin (McKeown-Longo and Mosher, 1983, 1984, 1985; Allio and McKeown-Longo, 1988). Pulse chase experiments indicate that fibronectin binds initially in the deoxycholate soluble fraction and is transferred to the deoxycholate insoluble fraction (McKeown-Longo and Mosher, 1983; Barry and Mosher, 1989). Binding and transfer can be downregulated with cholera toxin (Allen-Hoffmann and Mosher, 1987) and upregulated with transforming growth factor-beta (Allen-Hoffmann et al., 1988) or, in HT1080 tumor cells, with dexamethasone (McKeown-Longo and Etzler, 1987). Immunoelectron microscopy studies indicate that the amino-terminal fragment of fibronectin binds to the cell surface of fibroblasts like the intact molecule, but does not colocalize with fragments of fibronectin containing the cell adhesion sites (Peters and Mosher, 1987). Assembly of fibronectin fibrils therefore appears to occur at sites that are distinct from or more complex than the cell attachment receptor (Pierschbacher et al., 1983; Pytela et al., 1985; Ruoslahti and Pierschbacher, 1987). Soluble fibronectin, however, seems to interact with itself during formation of the fibronectin fibrils and can bind directly to matrix (Chernousov et al., 1985; Barry and Mosher, 1989).

In this paper, we examined the binding and incorporation of exogenous pFN and endogenous cFN in human skin fibroblast cultures using fluorescent and immunoelectron microscopy. In the fluorescent microscopy studies, fibroblast cultures were incubated with pFN labeled with FITC and then labeled with a monoclonal antibody specific for the EIIIA sequence found in cFN (Borsi et al., 1987). The antibody specific for cFN was localized using a rhodamine-conjugated goat anti-mouse IgG. Electron microscopy studies used a goat anti-rabbit IgG bound to 18-nm gold beads to detect rabbit antifluorescein antibodies reacting with FITC-pFN. A goat anti-mouse IgG coupled to 5-nm gold beads localized the monoclonal antibody specific for EIIIA in the electron microscopy studies. These studies show that exogenously added pFN binds to regions of the cell surface where cFN is also localized, but does not need to bind to cFN to enter the matrix. In addition, these studies show that in a fibronec-

1. *Abbreviations used in this paper*: cFN, cellular fibronectin; pFN, plasma fibronectin.

tin fibril composed of pFN and cFN, pFN and cFN are localized in discrete patches along the fibril.

Materials and Methods

Cell Culture and Labeling Conditions

Neonatal human foreskin fibroblasts were either grown in Ham's F-12 medium or Ham's F-12 and DME (1:1 ratio) supplemented with 10% FBS.

Fibroblasts used in immunofluorescent studies were plated at a density of 3×10^5 cells onto glass coverslips in 35-mm dishes and grown for either 18 or 42 h at 37°C. Cycloheximide (25 μg/ml) was added to some of the cultures after 1 h. FITC-pFN (20 μg/ml or 250 μg/ml) was applied to some cultures 2 h after plating. In other experiments, fibroblasts were grown for 18 or 42 h, then washed and treated with cycloheximide (25 μg/ml) for 1 h. FITC-pFN was added to the cycloheximide-containing medium, and the cells were incubated for an additional 4 h.

For immunoelectron microscopy studies, fibroblasts were seeded onto formvar-coated gold grids on glass coverslips (Wolosewick and Porter, 1976) precoated with 160–180-kD cell attachment fragments of fibronectin (Williams et al., 1983; McKeown-Longo and Mosher, 1985). Fibroblasts were allowed to attach for 3 h before the fibroblasts were treated with 25 μg/ml cycloheximide for 18 h at 37°C. Some of the fibroblasts were then incubated with 20 μg/ml FITC-pFN for 3 h at 37°C.

Preparation of FITC-pFN and Colloidal Gold Antibody Complexes

Plasma fibronectin was purified as described by Mosher and Johnson (1983). FITC-pFN was prepared using the procedure of McKeown-Longo and Mosher (1983). Spectroscopy measurements at 280 and 495-nm indicated that the labeled protein contained ~3 FITC/subunit of fibronectin.

Colloidal gold beads 18 nm in diameter (Au_{18}) were prepared by reducing gold chloride with trisodium citrate as described by Geoghegan and Ackerman (1977). Colloidal gold beads 5 nm in diameter (Au_5) were prepared by reducing gold chloride with white phosphorus as described by DeMay (1983).

Polyclonal antibodies to rabbit IgG and mouse IgG (Jackson Laboratory, Bar Harbor, ME) were coupled to Au_{18} and Au_5 beads, respectively, at pH 9.0 using the procedure described by DeMay (1983). The minimal concentration of IgG necessary to stabilize 1 ml of the gold sol was determined using an absorption isotherm (Horisberger and Rosset, 1977). Unbound areas on the gold beads were blocked with 1% BSA, pH 9.0.

Immunofluorescent Microscopy

Fibroblasts were washed three times with 10 mM sodium phosphate (pH 7.4) containing 150 mM sodium chloride and fixed for 30 min with 3.5% paraformaldehyde in 0.1 M sodium phosphate (pH 7.4). Fixed cells were labeled for 30 min with either a monoclonal antibody (IST-9) to the EIIIA domain of cFN or a monoclonal antibody (IST-7) to an adjacent region of fibronectin (Borsi et al., 1987). Ascites containing the antibodies was used at a dilution of 1:1,000 in 1% BSA in PBS. Cells were washed three times and then labeled with rhodamine-conjugated goat anti-mouse IgG in 1% ovalbumin in PBS for 45 min.

Immunoelectron High Voltage Electron Microscopy

Fibroblasts were washed three times with Hank's balanced salt solution (HBSS), prefixed with 0.1% glutaraldehyde, 0.1 M Hepes, pH 7.0, and treated with sodium borohydride (0.5 mg/ml), 0.1 M Hepes, pH 7.0, for 10 min. Prefixed fibroblasts were labeled with rabbit antifluorescein serum (1:100 dilution), and mouse IST-9 ascites (1:100 dilution). The labeling was for 1 h at 23°C in 20 mM Tris-HCl, pH 8.2, containing 150 mM sodium chloride, 20 mM sodium azide and 1% BSA. Cells were washed three times with the same buffer and then incubated for 1 h at room temperature with anti-rabbit IgG and anti-mouse IgG antibodies conjugated to Au_{18} and Au_5 gold beads, respectively, in the 20 mM Tris-HCl (pH 8.2), 150 mM NaCl buffer contains 20 mM sodium azide and 1% BSA. The fibroblasts were washed with 20 mM Tris-HCl (pH 8.2), containing 150 mM sodium chloride and 20 mM sodium azide and prepared for electron microscopy as described previously (Peters and Mosher, 1987).

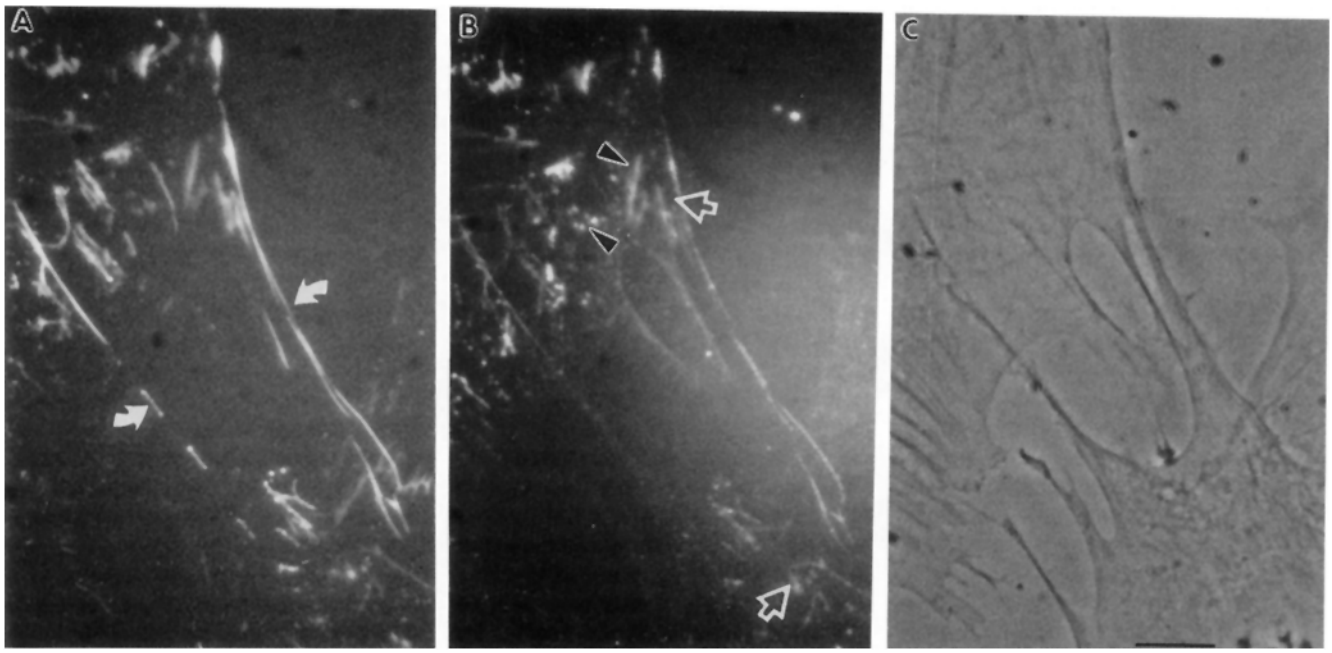

Figure 1. Deposition of FITC-pFN in the presence of a preexisting cFN matrix. Cells were grown for 42 h, incubated with cycloheximide (25 μg/ml) for 1 h, and then incubated for 4 h with cycloheximide and 250 μg/ml FITC-pFN. Cells were fixed, labeled with IST-9 antibody and then labeled with a rhodamine-conjugated goat anti-mouse antibody. (*A*) FITC-pFN is observed in short fibrils along the retracting edges of the cell (*arrows*). The exogenous FITC-pFN appears to fill in areas along fibrils where little cFN had been deposited (*arrows*). (*B*) Immunofluorescence of the fibroblast in *A*. cFN is observed in patches and fibrils (*arrowheads*). cFN is also observed in fibrillar networks that colocalize with FITC-pFN (*open arrowheads*). (*C*) Phase micrograph of *A* and *B*. Bar, 13.3 μm.

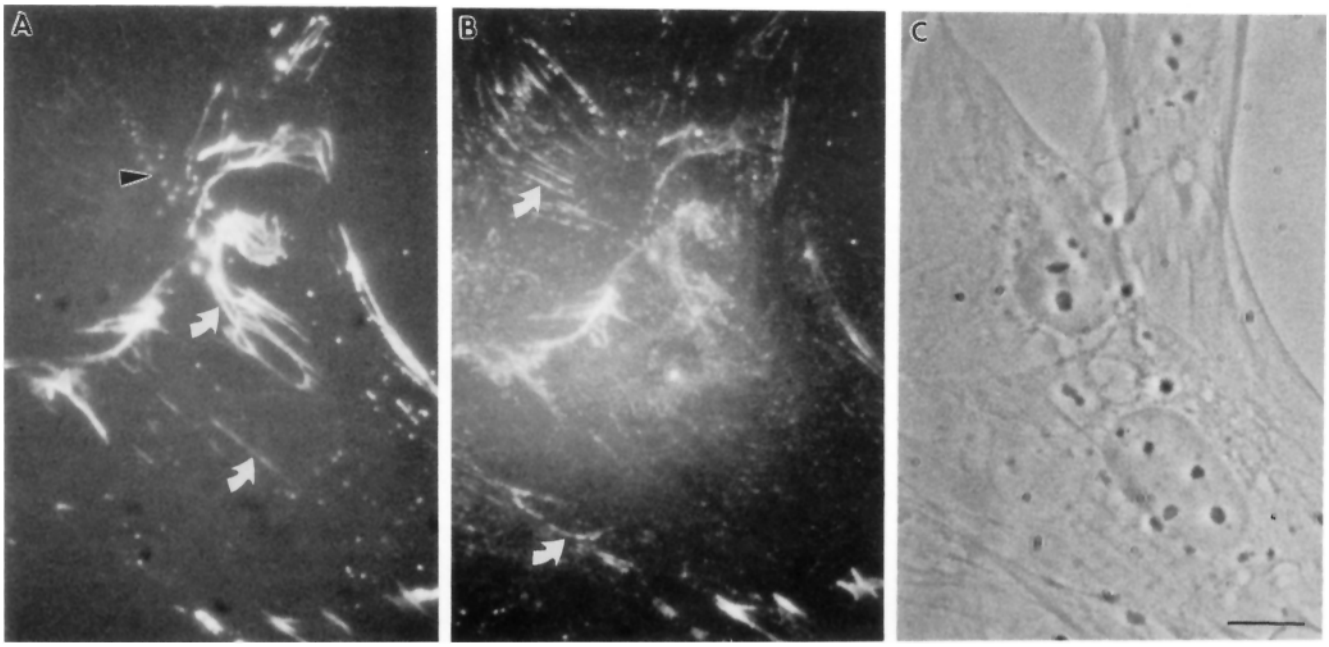

Figure 2. Deposition of endogenous FN in cells with a preexisting matrix of FITC-pFN. Cells were allowed to settle for 1 h and then treated with cycloheximide (25 μg/ml). After 1 h in cycloheximide, FITC-pFN (20 μg/ml) was added. The cells were incubated for 18 h, washed free of cycloheximide and FITC-pFN, placed in fresh medium, and incubated for an additional 3 h at 37°C to allow synthesis and deposition of cFN. Cells were fixed and labeled with IST-9 to cFN as described in Fig. 1. (*A*) FITC-pFN is observed in a punctate pattern (*arrowheads*) and in short fibrils on the cell surface (*arrows*). (*B*) Immunofluorescence of the fibroblast in *A*. Areas where there is no colocalization between FITC-pFN and cFN can be observed (*arrows*). (*C*) Phase micrograph of *A* and *B*. Bar, 13.3 μm.

Morphometric Analysis

Micrographs of extracellular matrix fibrils were randomly chosen from 25 different areas for each of the three experimental conditions analyzed. The distribution of 5- and 18-nm gold beads along the length of fibrils (2.0 μm) was determined by counting the number of gold beads found in consecutive 60-nm segments along the fibril. The length of each region along the fibril containing either cFN or pFN was determined using an IBM-XT computer and the Morphometer program (Woods Hole Educational Associates, Woods Hole, MA). The Sigmaplot program (Jandel Scientific, Corte Madera, CA) and Surfer Program (Golden Software, Golden, CO) were used to further analyze and graph the data.

Results

Double fluorescent microscopic studies of fibroblasts cultured for 18 or 42 h and then treated with cycloheximide and FITC-pFN showed that pFN does not necessarily bind to cFN on the cell surface (Fig. 1). The lack of colocalization was more marked in cultures incubated with 250 μg/ml of FITC-pFN than with 20 μg/ml FITC-pFN. FITC-pFN was observed bound to the retracting edges of fibroblast surface along regions of the cell where very little cFN had previously been laid down (*arrows*). FITC-pFN was also observed bound to regions of the cell where cFN had previously been deposited (*open arrows*). Regions where only cFN existed were also observed (*small arrowheads*).

The converse experiment was done in which fibroblast cultures were grown for 18 h in cycloheximide in the presence of FITC-pFN followed by incubation in the absence of exogenous FITC-pFN and cycloheximide (Fig. 2, *A–C*). In these cultures, FITC-pFN was found predominantly in linear arrangements. The newly synthesized cFN did not always colocalize with the FITC-pFN and appeared on the cell surface in arrays or patches (*arrow*).

A number of controls were done. If cells were incubated with FITC-pFN in the absence of cycloheximide, FITC-pFN and cFN colocalized at the fluorescent microscopic level with the exception of patches of cFN that were observed between the cells and coverslip. Under experimental conditions in which FITC-pFN did not colocalize with IST-9, FITC-pFN did colocalize with IST-7, a monoclonal antibody that does not distinguish between cFN and pFN.

Fibroblasts incubated with or without FITC-pFN (20 μg/ml) in the presence or absence of cycloheximide were prepared by similar protocols and examined by high voltage electron microscopy.

Fig. 3 *A* shows a fibroblast that had been grown for 24 h in the absence of cycloheximide and FITC-pFN and then labeled with IST-9 and anti-FITC. Cellular fibronectin (5-nm beads) is observed on the cell surface along stress fibers at the retracting end of the fibroblast and in fibrils in the extracellular space. Only an occasional 18-nm gold bead marking FITC-pFN is observed (also see Fig. 6). Presumably, this represents nonspecific binding of the anti–rabbit IgG-gold conjugate.

When FITC-pFN was added in the absence of cycloheximide, both cFN and FITC-pFN were observed distributed together in linear arrangements along the lateral and retracting edges of the fibroblast surface (Fig. 3 *B*). However, there was not complete admixture of the two labels suggesting that the FITC-pFN was not binding to cFN on the cell surface (Fig. 3 *C*).

When fibroblasts were incubated with FITC-pFN in the presence of cycloheximide and then labeled with anti-FITC and IST-9, FITC-pFN was observed bound to the cell surface in linear arrangements along the lateral and retracting edges of the fibroblast (Fig. 4 *A*). The markers for cFN on the cell

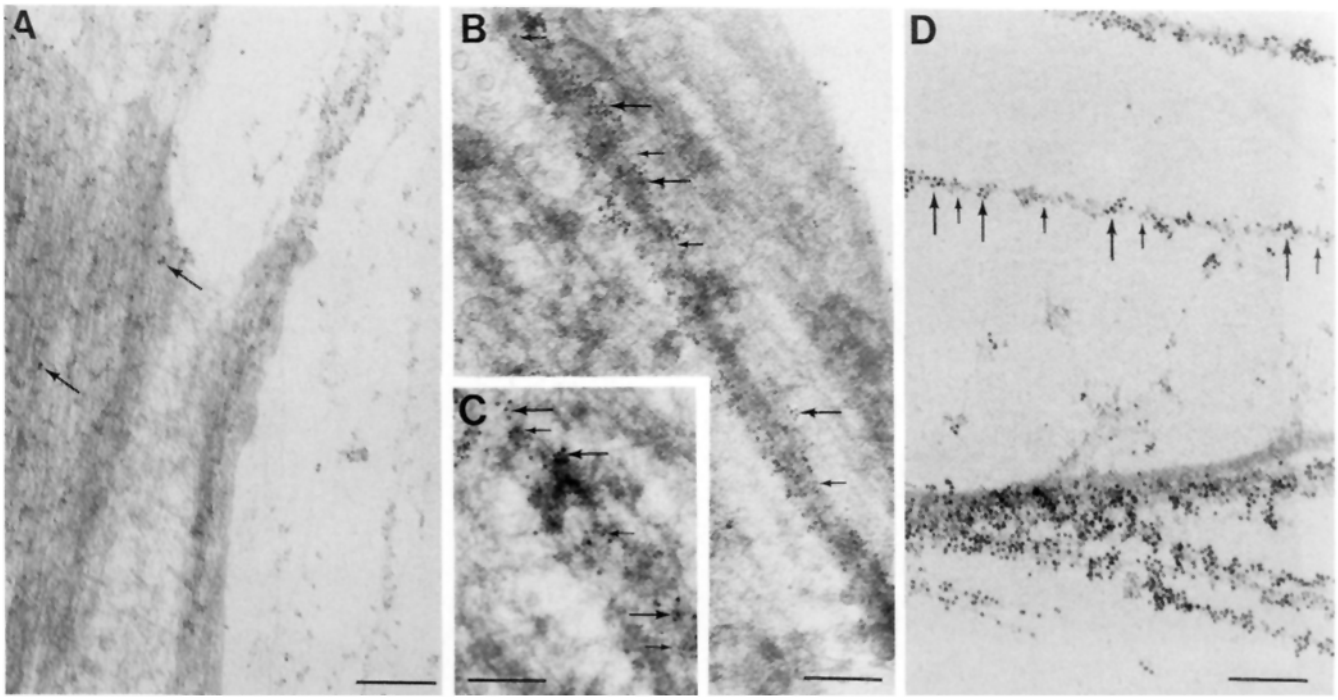

Figure 3. Immunoelectron micrographs of fibroblasts grown in the presence and absence of FITC-pFN. Cells were labeled for FITC-pFN (18-nm beads) and cFN (5-nm beads) as described in Material and Methods. (*A*) Whole mount of fibroblast grown for 24 h in the absence of FITC-pFN. Cellular fibronectin localizes with bundles of microfilaments along the retracting edge of the fibroblast. It can also be observed in extracellular matrix fibrils. Occasionally 18-nm gold beads are present (*arrows*). Bar, 0.25 μm. (*B*) Whole mount of fibroblast grown for 24 h in the presence of FITC-pFN. Both cFN (*small arrows*) and FITC-pFN (*large arrows*) is observed in linear arrangements above bundles of microfilaments along the lateral edge of the fibroblast. Bar, 0.26 μm. (*C*) Higher magnification of cell treated as described in *B*. Although both cFN and FITC-pFN are observed in the same vicinity, there appear to be discrete localized concentrations of each. Bar, 0.20 μm. (*D*) Immunoelectron micrograph of extracellular matrix from cultures incubated with FITC-pFN. Both cFN (*arrowheads*) and FITC-pFN (*arrows*) are observed grouped into separate clusters along the same fibrils. The impression that the clusters were binding to the same fibrils was confirmed by examination of stereo pairs. Bar, 0.25 μm.

surface were reduced markedly compared to cells not incubated in cycloheximide. What little cFN was observed on the cell surface did not appear to colocalize with FITC-pFN (Fig. 4 *B*). Fibrils composed primarily of FITC-pFN were observed in the extracellular space (also see Fig. 6).

To verify the specificities of the labeling patterns, fibroblasts that had never been incubated with FITC-pFN and had been cultured in the presence of cycloheximide were labeled with anti-FITC and IST-9 antibodies. These cells did not show any labeling (Fig. 4 *C*). Fibroblasts incubated without primary antibodies to FITC and cFN also showed no labeling (not shown).

The pattern of cFN and FITC-pFN in fibrils that contain both fibronectins was distinctive (Fig. 3 *D*). FITC-pFN (*arrows*) and cFN (*arrowheads*) were grouped into discrete regions of the fibrils so that one area contained predominantly labels for cFN and an adjacent region contained labels for FITC-pFN. Fig. 5 *A* shows the distribution of FITC-pFN and cFN in consecutive 60-nm segments of the fibril in Fig. 5 *B*. It is apparent that whenever FITC-pFN (*open circles*) is observed, cFN (*closed circles*) is usually not observed and vice versa. There are only three places (*arrows*) along the fibril (2.0 μm in length) where cFN and FITC-pFN colocalize.

Several additional quantitative analyses were done on fibrils containing both cFN and FITC-pFN, fibrils containing mostly cFN, and fibrils containing mostly FITC-pFN. Fig. 6, *A–C*, shows the average numbers of 5- and 18-nm gold beads found in consecutive 60-nm segments along the length of these three types of matrix fibrils. In fibrils grown in the absence of cycloheximide and FITC-pFN and therefore containing mostly cFN (Fig. 6 *A*), only an occasional 18-nm gold bead (corresponding to FITC-pFN) was found. Likewise, in fibrils from cultures grown in the presence of cycloheximide and FITC-pFN and therefore containing mostly FITC-pFN, only an occasional 5-nm gold (corresponding to cFN) was found (Fig. 6 *B*). When the average number of 5- and 18-nm beads were analyzed in fibrils containing both FITC-pFN and cFN, both labels are found throughout the length of the fibrils. The average numbers of the two labels in the three types of fibronectin fibrils are plotted against one another in Fig. 7. The points are divided into three groups and do not overlap with one another.

Individual measurements from 60-nm segments along fibrils containing both cFN and FITC-pFN were plotted on a contour plot (Fig. 8; compare to Fig. 7). Few of the segments contained both 5- and 18-nm gold beads. Instead, individual segments contained mainly 5- or 18-nm gold beads, as was found in fibrils containing only cFN or FITC-pFN.

Discussion

The immunoelectron microscopy studies together with the fluorescence studies show that FITC-pFN is treated like cFN

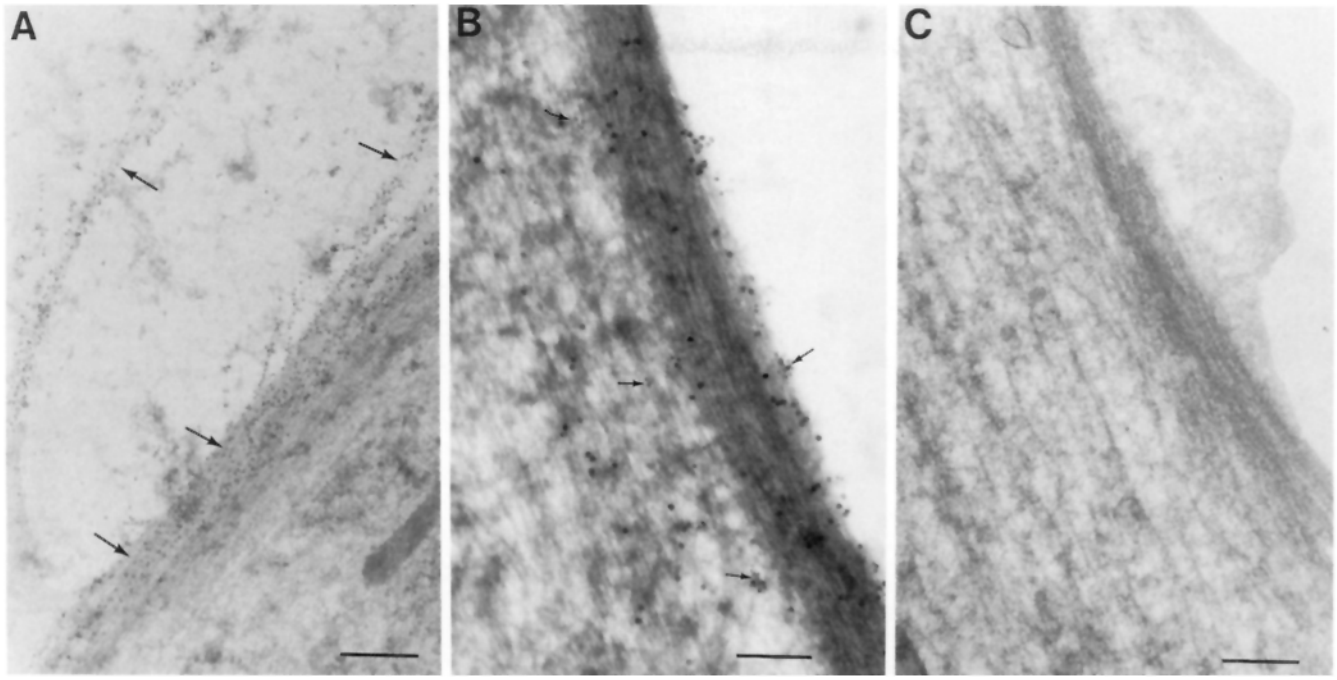

Figure 4. Immunoelectron micrographs of fibroblasts grown in the presence of cycloheximide. Cells were labeled as described for Fig. 3. (*A*) Whole mount of fibroblast. Cycloheximide (25 μg/ml) was added 3 h after seeding. Cells were grown at 37°C for an additional 18 h. Afterwards, FITC-pFN (20 μg/ml) was added, and the cells were incubated for an additional 3 h. FITC-pFN (18-nm beads) is observed along the lateral edges of the fibroblast and in extracellular matrix fibrils (*arrows*). The FITC-pFN on the cell surface colocalizes along bundles of microfilaments. Bar, 0.41 μm. (*B*) Higher magnification of cell treated as described in *A*. Occasionally, cFN (*arrows*) are observed on the cell surface or in matrix fibrils. Bar, 0.16 μm. (*C*) Whole mount of fibroblast cultured with cycloheximide and no FITC-pFN. Neither 18- or 5-nm beads are observed on the cell surface. Bar, 0.41 μm.

by cultured fibroblasts. Both FITC-pFN and cFN were found bound to the cell surface along specific regions of the cell. These regions that occur primarily along the lateral and retracting edges of the fibroblast cell surface were shown previously to represent sites involved in the fibrillogenesis of fibronectin-gold complexes (Peters and Mosher, 1987).

Our results support recent evidence (McKeown-Longo and Etzler, 1987; Allen-Hoffmann et al., 1988) that exogenous pFN can bind to the cell layer and become incorporated into the extracellular matrix of cells with blocked protein synthesis. This finding suggests that molecules on the cell surface involved in fibronectin binding and matrix assembly have a long half-life. It also demonstrates that pFN-cFN interactions are not needed for the binding of exogenous pFN to the cell surface. The immunoelectron microscopy studies further show that FITC-pFN was assembled into an extensive matrix within 3 h in the cycloheximide-treated cultures. Thus, pFN seems to contain all the structures needed for fibril assembly.

The deposition of pFN in the matrix of cultured fibroblasts has been shown to be dependent on the concentration of pFN used. Half maximal rates of incorporation (K_m) are achieved at about 25 μg/ml (Allen-Hoffmann et al., 1988; Barry and Mosher, 1988). The matrix itself contains binding sites for pFN which seem to be nonsaturable (Chernousov et al., 1985; Peters and Mosher, 1987). By fluorescence microscopy of 18- or 48-h cultures pretreated with cycloheximide for 1 h and then incubated with FITC-pFN, the FITC-pFN colocalized with preexisting fibrillar cFN and also appeared to form new fibrils not containing cFN. The new fibrils were detected more easily in cultures incubated with 250 μg/ml FITC-pFN (the plasma concentration but 10-fold higher than the estimated K_m of incorporation) than in cultures incubated with 20 μg/ml FITC-pFN. This may be because the higher concentrations of FITC-pFN competed for or excluded the trace amounts of cFN secreted by cycloheximide-treated cells (estimated by immunoassay of medium to be ~5% of nontreated cells). At the electron microscopic level, when cultures were treated with cycloheximide 3 h after plating, little cFN was found in fibrils of cycloheximide-treated cultures.

The deposition of bulk cFN in medium appears to follow the same rules as deposition of pFN (Allio and McKeown-Longo, 1988). There appeared, however, to be regions of the ventral cell surface where cFN was deposited preferentially. We speculate that cFN may be vectorially secreted to regions of the cell surface able to assemble fibronectin or into restricted volumes in which cFN is preferentially assembled.

Our most intriguing finding is that when FITC-pFN and cFN coassemble into fibrils, the fibrils have regions enriched in one of the two forms. This finding could be due to vectorially or temporally regulated secretion; e.g., pulses of cFN secretion into assembly sites. We favor, however, the explanation that the orientation of fibronectin in fibrils may impose certain structural requirements that encourage cFN to bind preferentially to cFN and pFN to bind to pFN. As shown in Fig. 9, subunits containing EIIIA and/or EIIIB may preferentially interact with one another leading to an area

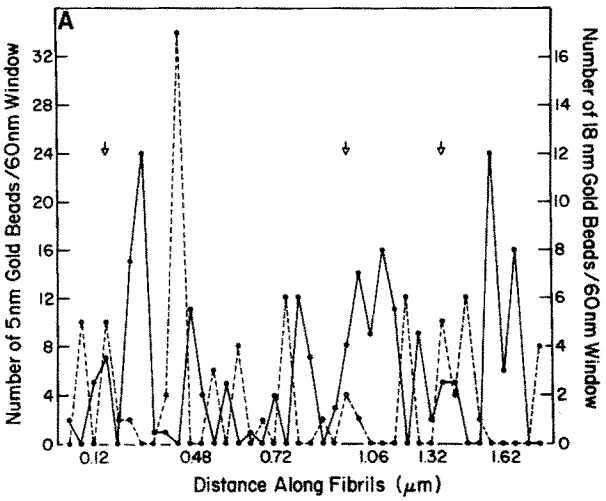

Figure 5. Distribution of cFN and FITC-pFN in matrix fibrils. (*A*) Graphic representation of FN fibril shown in *B*. Closed circles denote cFN; open circles denote FITC-pFN. Arrows denote areas where discrete patches of cFN and FITC-pFN are not apparent. (*B*) Immunoelectron micrograph of fibronectin fibril (2.0 μm in length). FITC-pFN (large gold beads) and cFN (small gold beads) are grouped in discrete patches along the fibril. Arrowheads denote areas where discrete patches are not apparent. Bar, 0.16 μm. When data from 25 randomly chosen fibrils were analyzed, it was found that the patches of cFN and FITC-pFN varied in length from 9 to 812 nm for cFN and 28 to 1,200 nm for FITC-pFN. The average lengths of these patches were 152 nm for cFN and 172 nm for FITC-pFN. There are regions where no label is observed. This is presumably due to the fact that the IST-9 antibody recognizes only cFN molecules that have EIIIA inserts.

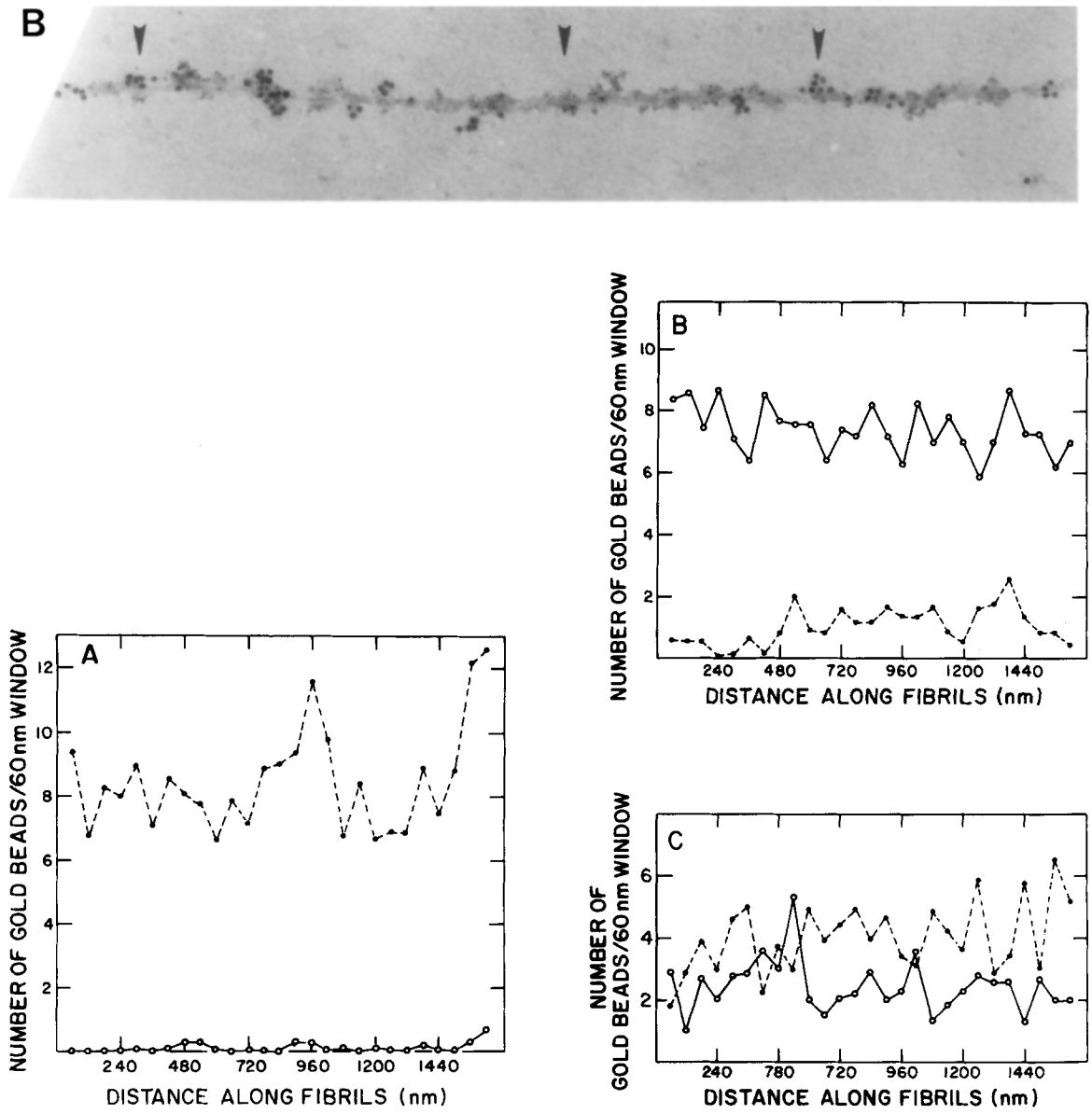

Figure 6. Average numbers of 5- and 18-nm gold beads observed along 60-nm segments of FN fibrils. Cells grown in (*A*) the absence of cycloheximide and FITC-pFN; (*B*) the presence of cycloheximide and FITC-pFN; or (*C*) the absence of cycloheximide and the presence of FITC-pFN. Open circles represent FITC-pFN; closed circles represent cFN. The distribution of the labels in *C* indicates that each segment has the potential to contain cFN and FITC-pFN (see also Fig. 7).

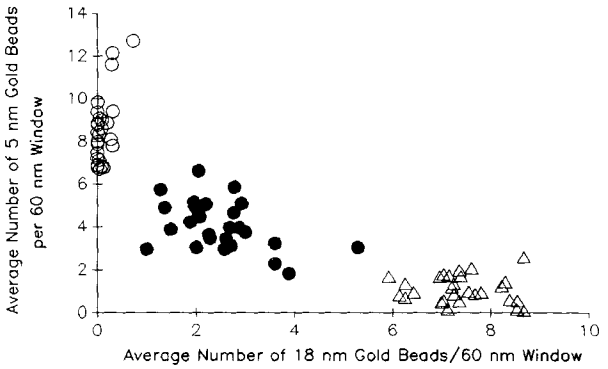

Figure 7. Plot of the average number of 5-nm gold beads (cFN) versus 18-nm gold beads (FITC-pFN) found in 60-nm segments of FN fibrils. Open circles represent data from cells grown in the absence of cycloheximide and FITC-pFN; closed circles represent data from cells grown in the presence of FITC-pFN; open data from triangles represent data from cells grown in the presence of cycloheximide and FITC-pFN.

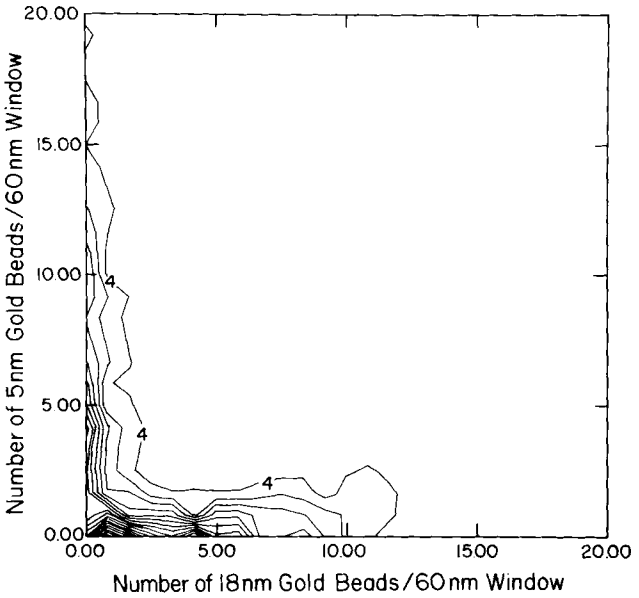

Figure 8. Contour plot showing the distribution of numbers of 18-nm (FITC-pFN) and 5-nm (cFN) beads in individual 60-nm segments among fibrils containing both cFN and FITC-pFN. The majority of 60-nm segments were enriched in either cFN or FITC-pFN (compare to average values shown in Fig. 7, *closed circles*). Measurements from 25 randomly chosen fibrils were plotted, N = 876. The number 4 represents the frequency with which data points are observed along that contour line.

that is enriched in cFN and poor in FITC-pFN. Conversely, FITC-pFN may assemble with itself unless it encounters a heterodimeric cFN consisting of one subunit with the EIIIA/B sequences and a second subunit lacking the EIIIA/B sequences. Such preferential binding and assembly would insure that cells induced to secrete certain isoforms of fibronectin, as happens with growth factor stimulation (Balza et al., 1988) or during embryogenesis (ffrench-Constant and Hynes, 1988) and wound healing (ffrench-Constant et al., 1989), are able to populate their matrix with the secreted isoforms despite the presence of other isoforms of fibronectin.

The data presented in this manuscript do not enable us to predict the exact interactions between neighboring fibronectin molecules. Fig. 9 assumes a simple head-to-tail interaction of subunits. Further studies need to be done to determine the three-dimensional structure of fibronectin-containing fibrils and the exact sites of polymerization.

We thank Dr. Luciano Zardi for generously providing us with the monoclonal antibody (IST-9) used in these experiments.

This work was supported by grants HL21644 (to D. F. Mosher) and AR37052 (to D. P. Peters) from the National Institutes of Health. This work was also supported by a General Research Grant to D. P. Peters from the University of Wisconsin Medical School.

Received for publication 17 March 1989 and in revised form 6 March 1990.

References

Allen-Hoffmann, B. L., and D. F. Mosher. 1987. Matrix assembly sites for exogenous fibronectin are decreased on human fibroblasts after treatment with agents which increase intracellular cAMP. *J. Biol. Chem.* 262:14361–14365.

Allen-Hoffmann, B. L., C. L. Crankshaw, and D. F. Mosher. 1988. Transforming growth factor-β increases cell surface binding and assembly of exogenous (plasma) fibronectin by normal human fibroblasts. *Mol. Cell Biol.* 8:4234–4242.

Allio, A. F., and P. J. McKeown-Longo. 1988. Extracellular matrix assembly of cell-derived and plasma-derived fibronectins by substrate attached fibroblasts. *J. Cell Physiol.* 135:459–466.

Balza, E., L. Borsi, G. Allemanni, and L. Zardi. 1988. Transforming growth factor β regulates the levels of different fibronectin isoforms in normal human cultured fibroblasts. *FEBS (Fed. Eur. Biochem. Soc.) Lett.* 228:42–44.

Barry, E. L. R., and D. F. Mosher. 1988. Factor XIII cross-linking of fibronectin at cellular matrix assembly sites. *J. Biol. Chem.* 263:10464–10469.

Barry, E. L. R., and D. F. Mosher. 1989. Factor XIIIa-mediated cross-linking of fibronectin in fibroblast cell layers. Cross-linking of cellular and plasma fibronectin and amino-terminal fibronectin fragments. *J. Biol. Chem.* 264: 4179–4185.

Borsi, L., B. Carnemolla, P. Castellani, C. Rosellini, D. Vecchio, G. Allemanni, S. E. Chang, J. Taylor-Papadimitriou, H. Pande, and L. Zardi. 1987. Monoclonal antibodies in the analysis of fibronectin isoforms generated by alternative splicing of mRNA precursors in normal and transformed human cells. *J. Cell Biol.* 104:595–600.

Chernousov, M. A., M. L. Metsis, and V. F. Koteliansky. 1985. Studies of extracellular fibronectin matrix formation with fluoresceinated fibronectin and fibronectin fragments. *FEBS (Fed. Eur. Biochem. Soc.) Lett.* 183: 365–369.

DeMey, J. 1983. Colloidal gold probes in Immunocytochemistry. *In* Immuno-

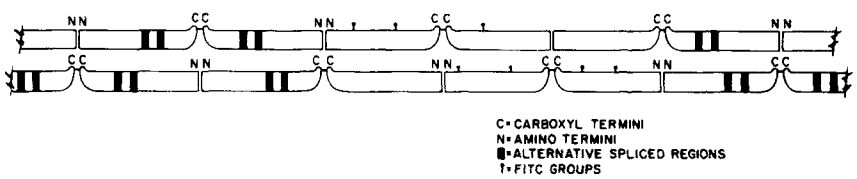

Figure 9. Proposed arrangement of cFN and pFN molecules arranged in a fibril. Heterodimeric and homodimeric cFN molecules are distinguished by having extra domains in one and both subunits, respectively. Fibril formation is hypothesized to be driven by reciprocal interactions between the subunits of different fibronectin molecules. Such reciprocal interactions are possible only if the interacting subunits are of the same type and would result in facile disulfide multimer formation. Thus, only heterodimeric cFN can interact with FITC-pFN lacking extra domains. The model would be more complex if one distinguished among all the possible splice variants.

cytochemistry Practical Applications in Pathology and Biology. J. M. Polak and S. Van Noorden, editors. Wright-PSG, Boston. 82–112.

ffrench-Constant, C., and R. O. Hynes. 1988. Patterns of fibronectin gene expression and splicing during cell migration in chicken embryos. *Development (Camb.).* 104:369–382.

ffrench-Constant, C., L. Van de Water, H. F. Dvorak, and R. O. Hynes. 1989. Reappearance of an embryonic pattern of fibronectin splicing during wound healing in the adult rat. *J. Cell Biol.* 109:903–914.

Geoghegan, W. D., and A. Ackerman. 1977. Absorption of horseradish peroxidase, ovomucid, and anti-immunoglobulin to colloidal gold for the indirect detection of concanvalin A, wheat germ agglutinin and goat anti-human immunoglobulin G on cell surfaces at the electron microscopic level: a new method, theory and application. *J. Histochem. Cytochem.* 25:1187–1200.

Gutman, A., and A. R. Kornblihtt. 1987. Identification of a third region of cell-specific alternative splicing in a human fibronectin mRNA. *Proc. Natl. Acad. Sci. USA.* 84:7179–7182.

Hayman, E. G., and E. Ruoslahti. 1979. Distribution of fetal bovine serum fibronectin and endogenous rat cell fibronectin in extracellular matrix. *J. Cell Biol.* 83:255–259.

Horisberger, M., and J. Rosset. 1977. Colloidal gold, a useful marker for transmission and scanning electron microscopy. *J. Histochem. Cytochem.* 25: 295–305.

Kornblihtt, A. R., K. Vibe-Pedersen, and F. E. Baralle. 1984. Human fibronectin: molecular cloning evidence for two mRNA species differing by an internal segment coding for a structural domain. *EMBO (Eur. Mol. Biol. Organ.) J.* 3:221–226.

Kornblihtt, A., K. Umezawa, K. Vibe-Pedersen, and F. E. Baralle. 1985. Primary structure of human fibronectin: differential splicing may generate at least 10 polypeptides from a single gene. *EMBO (Eur. Mol. Biol. Organ.) J.* 4:1755–1759.

McDonald, J. A., B. J. Quade, T. J. Broekelmann, R. LaChance, K. Forsman, E. Hasegawa, and S. Akiyama. 1987. Fibronectin's cell-adhesive domain and an amino-terminal matrix assembly domain participate in its assembly into fibroblast pericellular matrix. *J. Biol. Chem.* 262:2957–2967.

McKeown-Longo, P. J., and D. F. Mosher. 1983. Binding of plasma fibronectin to cell layers of human skin fibroblasts. *J. Cell Biol.* 97:466–472.

McKeown-Longo, P. J., and D. F. Mosher. 1984. Mechanism of formation of disulfide-bonded multimers of plasma fibronectin in cell layers of cultured human fibroblasts. *J. Biol. Chem.* 259:12210–12215.

McKeown-Longo, P. J., and D. F. Mosher. 1985. Interaction of the 70,000 molecular weight amino terminal fragment of fibronectin with the matrix-assembly receptor of fibroblasts. *J. Cell Biol.* 100:364–374.

McKeown-Longo, P. J., and C. A. Etzler. 1987. Induction of fibronectin matrix assembly in human fibrosarcoma cells by dexamethasone. *J. Cell Biol.* 104:601–610.

Mosher, D. F., and R. B. Johnson. 1983. In vitro formation of disulfide-bonded fibronectin multimers. *J. Biol. Chem.* 258:6595–6601.

Oh, E., M. Pierschbacher, and E. Ruoslahti. 1981. Deposition of plasma fibronectin in tissues. *Proc. Natl. Acad. Sci. USA.* 78:3218–3221.

Peters, D. M., and D. F. Mosher. 1987. Localization of cell surface sites involved in fibronectin fibrillogenesis. *J. Cell Biol.* 104:121–130.

Pierschbacher, M. D., E. G. Hayman, and E. Ruoslahti. 1983. Synthetic peptides with cell attachment activity of fibronectin. *Proc. Natl. Acad. Sci. USA.* 80:1224–1227.

Pytela, R., M. D. Pierschbacher, and E. Ruoslahti. 1985. Identification and isolation of a 140 kD cell surface glycoprotein with properties expected of a fibronectin receptor. *Cell.* 40:191–198.

Quade, B. J., and J. A. McDonald. 1988. Fibronectin amino-terminal matrix assembly site is located within the 29 kDa amino-terminal domain containing five type I repeats. *J. Biol. Chem.* 263:19602–19609.

Roman, J., R. M. LaChance, T. J. Broekelmann, C. J. Kennedy, E. A. Wayner, W. G. Carter, and J. A. McDonald. 1989. The fibronectin receptor is organized by extracellular matrix fibronectin: implications for oncogenic transformation and for cell recognition of fibronectin matrices. *J. Cell Biol.* 108:2529–2543.

Ruoslahti, E., and M. D. Pierschbacher. 1987. New perspectives in cell adhesion: RGD and integrins. *Science (Wash. DC).* 238:491–497.

Schwarzbauer, J. E., J. W. Tamkun, I. R. Lemischka, and R. O. Hynes. 1983. Three different fibronectin mRNAs arise by alternative splicing within the coding region. *Cell.* 35:421–431.

Schwarzbauer, J. E., R. S. Patel, D. Fonda, and R. O. Hynes. 1987*a*. Multiple sites of alternative splicing of the rat fibronectin gene transcript. *EMBO (Eur. Mol. Biol. Organ.). J.* 6:2573–2580.

Schwarzbauer, J. E., R. C. Mulligan, and R. O. Hynes. 1987*b*. Efficient and stable expression of recombinant fibronectin polypeptides. *Proc. Natl. Acad. Sci. USA.* 84:754–758.

Williams, E. C., P. A. Janmey, J. D. Ferry, and D. F. Mosher. 1983. Fibronectin: effect of disulfide bond reduction on its physical and functional properties. *J. Biol. Chem.* 257:14973–14978.

Wolosewick, J. J., and K. R. Porter. 1976. Stereo high voltage electron microscopy of whole cells of the human diploid line, WI-38. *Am. J. Anat.* 147:303–324.

Zardi, L., B. Carnemolla, A. Siri, T. E. Petersen, G. Padella, G. Sebastio, and F. E. Baralle. 1987. Transformed human cells produce a new fibronectin isoform by preferential alternative splicing of a previously unobserved exon. *EMBO (Eur. Mol. Biol. Organ.) J.* 6:2337–2342.